New procedure to measure simultaneously the surface tension and contact angle

S. Champmartin, A. Ambari, and J. Y. Le Pommelec

This paper proposes a new procedure to simultaneously measure the static contact angle and the surface tension of a liquid using a spherical geometry. Unlike the other existing methods, the knowledge of one of both previous parameters and the displacement of the sphere are not mandatory. The technique is based on the measurement of two simple physical quantities: the height of the meniscus formed on a sphere at the very contact with a liquid bath and the resulting vertical force exerted on this object at equilibrium. The meniscus height, whose exact value requires the numerical resolution of the Laplace equation, is often estimated with an approximate 2D model, valid only for very large spheres compared to the capillary length. We develop instead another simplified solution of the Young-Laplace equation based on the work of Ferguson for the meniscus on a cylinder and adapted for the spherical shape. This alternative model, which is less restrictive in terms of the sphere size, is successfully compared to numerical solutions of the complete Young-Laplace equation. It appears to be accurate for sphere radii larger than only two capillary lengths. Finally the feasibility of the method is experimentally tested and validated for three common liquids and two "small" steel spheres.

I. INTRODUCTION

Interfacial phenomena are ubiquitous in nature (ground water, oil reservoirs…) and several processes depend on the surface energy (coating, imbibition…). In the case of liquids, the surface energy is called the surface tension and is determined by the molecular interaction between the liquid molecules. When such a liquid is put into contact with a solid, if the surface energy is not too high, the liquid forms a drop with a finite contact angle which is determined by the competition between the solid-liquid, solid-vapor, and liquid-vapor energies. Indeed, except in very rare exceptions, the measurable parameters are thus the liquid surface tension and the contact angle of the liquid on the solid.[1–4] The contact angle is not independent of the surface tension but cannot be simply determined from the liquid surface tension and there is often a need to characterize both the contact angle of a liquid and its surface tension. The contact angle θ is defined as the angle between the tangents of the liquid-vapor and solid-liquid interfaces where the three phases join (triple line). According to the classical Young's equation,[5] θ depends only on the interfacial energies

$$\cos\theta = \frac{\sigma_{sv} - \sigma_{sl}}{\sigma}, \tag{1}$$

with σ the liquid-vapor surface energy, σ_{sv} and σ_{sl}, respectively, the solid-vapor and solid-liquid surface energies. From the viewpoint of thermodynamics, these energies represent the works to produce a unit surface of interface at constant temperature, pressure, and chemical potential. The value of θ gives a good indication of how well a liquid and a solid interact: low-energy solids such as polymers are generally poorly wetted by liquids which form droplets with a high contact angle value ($\theta \geq 90°$); high-energy solids such as metals and glass are surfaces on which most liquids wet spontaneously forming puddles with a low value of the contact angle ($\theta \leq 90°$). Besides the knowledge of θ is also necessary to predict the invasion of liquids in porous media or in solid surface finishing. Experimentally it is very hard to measure a unique value of θ because the contact angle at equilibrium is often subject to a hysteresis[6,7] of at least 10°. This phenomenon is the result of the surface structural heterogeneities (slight roughness, spatial inhomogeneities) and chemical contamination. The simplest means to obtain θ consists in using a goniometer to measure the contact angle at the triple line of a sessile drop on a solid plane surface.[8] This technique is known to be inaccurate and sensitive to the surface cleanliness. Most alternative techniques are based on the measurement of the force exerted by a meniscus on solid surfaces of various shapes and the knowledge of the surface tension σ is prerequisite.[9] The techniques to measure σ are also numerous and described in details in many textbooks:[4,10,11] capillary rise method, pendant drop method, stalagnometric method, maximum pressure bubble method, Wilhelmy or Du Noüy methods, capillary waves method[12,13]…. In most of these techniques, the knowledge of the contact angle is necessary beforehand or estimated to be zero.

In this work, we propose a simple technique to simultaneously determine θ and σ. The knowledge of both parameters at the same time is often required to reduce the influence of the variability of the thermodynamic conditions encountered in separated measurements. This new procedure is based on the measurement of two accessible physical quantities: the capillary force on a sphere, which can be directly given by a microbalance, and the height of the meniscus, which can be

easily obtained by image analysis. To the author's knowledge, the only attempts to determine θ and σ at the same time using a sphere were proposed by Scheludko[14] and Huh,[15] but their techniques necessitate pulling the sphere off the liquid in order to deform the meniscus and require to solve numerically the Laplace equation. In the present work, the sphere remains at a fixed position reducing the likely experimental errors on the vertical position of the sphere. Note that contrary to the other classical methods, any assumptions about the value of θ and σ are required. We use in this work a solid spherical surface because this simple shape presents several advantages: whereas the ring and plate form both menisci with complex profiles, a sphere does not, making it possible to calculate the equilibrium shape and the resulting force rigorously; the meniscus is axisymmetric, stable,[16] and free of discontinuities or end effects allowing an easy optical inspection of its height; the axisymmetric shape of the meniscus makes the numerical and/or semi-analytical resolution of the Young-Laplace equation relatively easier; in the plate and ring methods, the vertical alignment of the solid is much more critical than for a sphere (the sphere touches the liquid bath at only one point, whereas the base of the ring or of the plate must be perfectly parallel to the liquid level); the spherical shape is compact and has naturally the smallest surface-to-volume ratio, reducing the potential surface contamination issues; finally the experimental results show a noticeable reproducibility. In the following, we study the vertical force exerted by the capillary bridge on the sphere. This force depends on the height of the meniscus and two simplified models are proposed and discussed by comparing them to a numerical solution. Finally the accuracy of the method is discussed and the procedure is successfully validated experimentally.

II. THEORETICAL AND NUMERICAL ANALYSIS

Fig. 1 below presents the sketch of the problem. As soon as the sphere of radius b contacts the liquid, the latter rises onto the solid surface and forms at equilibrium an axisymmetric meniscus with a height z_0 above the level of the liquid bath. The triple line radius r_0 is related to the sphere radius b and to z_0 by a simple geometrical relation

$$r_0 = \sqrt{z_0(2b - z_0)}. \tag{2}$$

At the triple line, the tangents to the meniscus and to the vertical direction form an angle β_0. This virtual contact angle is related to the actual contact angle θ by

$$\beta_0 = \theta - \alpha. \tag{3}$$

α is the angle between the vertical direction and the tangent to the sphere at the triple line. This angle is a function of the meniscus height z_0 and of the sphere radius b

$$\tan\alpha = \frac{b - z_0}{\sqrt{z_0\,(2b - z_0)}}. \tag{4}$$

Due to the axial symmetry of the problem, the balance of the forces acting on the sphere in the horizontal directions is automatically satisfied (as is the balance of the torque in all directions) and the remaining vertical force exerted on the sphere is, after deduction of the weight of the sphere,

$$p = 2\pi r_0\sigma\cos\beta_0 + \rho g\pi z_0^2\left(b - \frac{2z_0}{3}\right). \tag{5}$$

This force is composed of two parts: the first one $2\pi r_0\sigma\cos\beta_0$ is the vertical projection of the capillary force with the virtual contact angle β_0. This contribution is also equal to the weight of the liquid contained in the outer part of the meniscus for $r > r_0$. The second contribution $\rho g\pi z_0^2(b - 2z_0/3)$ is the weight of the liquid volume in the inner part of the meniscus for $r < r_0$. This volume is the cylinder of radius r_0 and height z_0 reduced by the volume of the spherical cap of base radius r_0 and height z_0. If the contact angle θ is given, the measurement of the force p and of the height z_0 and the use of Eq. (5) are sufficient to determining the surface tension σ. Likewise if the surface tension is known, the measurement of p and of z_0

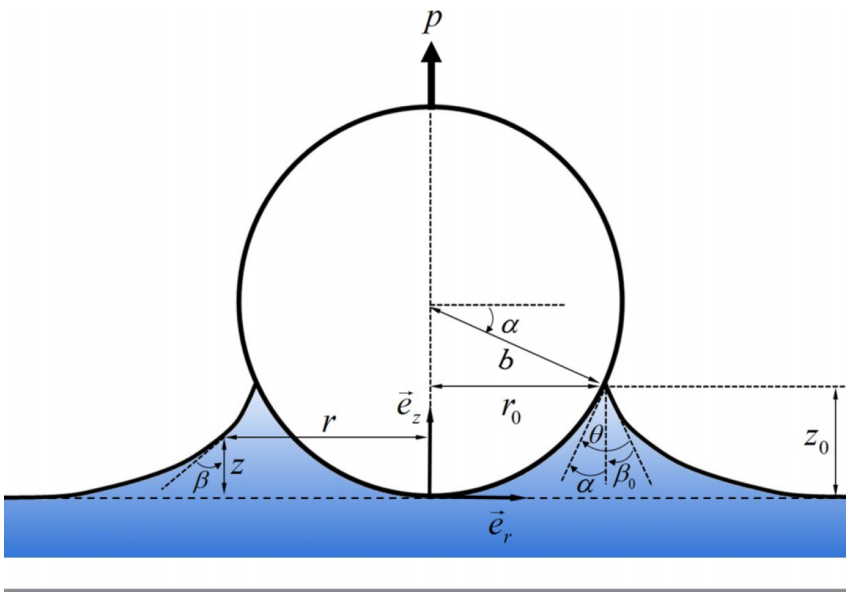

FIG. 1. Schematic representation of the meniscus on a sphere and notations.

gives access to the contact angle θ. In order to determine one of the parameters, the knowledge of the other one is needed as in the classical tensiometry techniques described in the Introduction. In order to overcome this dependence, another relation between z_0 and θ is required. This missing relation arises from the shape of the meniscus allowing to calculate the height z_0 of the liquid bridge at the triple line. This type of problems belongs to a class of mathematical issues studied by many authors.[17–19] The profile of the meniscus is a solution of the Young-Laplace equation

$$\sigma\left(\frac{1}{r_1}+\frac{1}{r_2}\right)=\rho g z, \tag{6}$$

with r_1 and r_2 the principal radii of curvature, ρ the liquid density, g the gravity constant, and z the vertical coordinate. In the present situation, the meniscus is axisymmetric and the previous equation in cylindrical coordinates becomes

$$\frac{\ddot{r}}{[1+\dot{r}^2]^{3/2}}-\frac{1}{r[1+\dot{r}^2]^{\frac{1}{2}}}=\frac{z}{a^2}, \tag{7}$$

with $a=\sqrt{\sigma/\rho g}$ the capillary length (the distance beyond which the gravity effects prevail over the capillary effects, typically around a few millimeters for most liquids), $\dot{r}=dr/dz$, and $\ddot{r}=d^2r/dz^2$. The boundary conditions are

$$\begin{cases}\text{for } r\to\infty : z=0, \dot{r}\to-\infty, & \text{(8a)}\\ \text{for } r=r_0 : z=z_0, \dot{r}_0=-\tan\beta_0. & \text{(8b)}\end{cases}$$

Eq. (7) has no analytical solution with the boundary conditions ((8a) and (8b)). However it is possible to obtain approximate solutions by means of some simplifications.

A. First approximation: 2D

When the sphere is large compared to the capillary length ($b \gg a$, large Bond or Eötvös numbers), the second term on the left-hand side of Eq. (7) is negligible. Indeed close to the triple line, we have $z_0 \sim a, r_1 \sim \sqrt{ab}$, and $r_2 \sim b$ implying that $1/r_2 \ll 1/r_1$. Then the Young-Laplace equation reduces to

$$\frac{\ddot{r}}{[1+\dot{r}^2]^{3/2}}=\frac{z}{a^2}. \tag{9}$$

This equation is valid when the axisymmetric curvature is negligible compared to the in-plane curvature. We can integrate Eq. (9) and using the boundary condition (8a), it gives

$$\frac{\dot{r}}{[1+\dot{r}^2]^{1/2}}=\frac{z^2}{2a^2}-1. \tag{10}$$

The meniscus height z_0 of the triple line at equilibrium is found using the second boundary condition (8b)

$$\frac{z_0^2}{2a^2}-1+\sin\beta_0=0. \tag{11}$$

This is of course the same relation as the one obtained for the capillary rise on a vertical plane or on a very large vertical or horizontal cylinder when the real contact angle is replaced by the virtual contact angle β_0. This 2D model is often used in the literature because of its simplicity but because the second curvature $1/r_2$ is completely neglected in this model, the solution (11) is expected to be accurate only for large spheres as we will confirm later.

B. Second approximation: Ferguson

In the case of the meniscus on a vertical cylinder, Ferguson[20] proposed to partially take into account the second curvature $1/r_2$. We adapt here his analysis in the case of the spherical surface, considering the latter as a stack of cylindrical slices. The term $1/\left[1+\dot{r}^2\right]^{1/2}$ in the second term on the left hand side of Eq. (7) is replaced using Eq. (10) of the previous 2D approximation

$$\frac{1}{[1+\dot{r}^2]^{1/2}}=\frac{1}{\dot{r}}\left(\frac{z^2}{2a^2}-1\right). \tag{12}$$

$\dot{r}$ is the slope of the profile of the meniscus at a given height z and is simply

$$\dot{r}=-\tan\beta=\frac{\sin\beta}{\sqrt{1-\sin^2\beta}}. \tag{13}$$

Using Eq. (11) we obtain

$$\dot{r}=-\frac{1-\frac{z^2}{2a^2}}{\frac{z}{a}\sqrt{1-\frac{z^2}{4a^2}}}. \tag{14}$$

Putting (14) into (12) gives

$$\frac{1}{\left[1+\dot{r}^2\right]^{1/2}}=\frac{z}{a}\sqrt{1-\frac{z^2}{4a^2}}. \tag{15}$$

The approximate Young-Laplace equation now writes

$$\frac{\ddot{r}}{\left[1+\dot{r}^2\right]^{3/2}}=\frac{z}{a^2}+\frac{z}{ra}\sqrt{1-\frac{z^2}{4a^2}}. \tag{16}$$

Supposing that the meniscus radius r is constant and of the order of the triple line radius r_0, we obtain

$$\frac{\ddot{r}}{\left[1+\dot{r}^2\right]^{3/2}}=\frac{z}{a^2}+\frac{z}{r_0 a}\sqrt{1-\frac{z^2}{4a^2}}. \tag{17}$$

This equation can be integrated, and using the boundary condition (8a), it gives

$$\frac{\dot{r}}{\left[1+\dot{r}^2\right]^{1/2}}=\frac{z^2}{2a^2}-1-\frac{4a}{3r_0}\left[\left(1-\frac{z^2}{4a^2}\right)^{3/2}-1\right]. \tag{18}$$

The height z_0 of the triple line is obtained again using second boundary condition (8b)

$$\frac{z_0^2}{2a^2}-1+\sin\beta_0=\frac{4a}{3r_0}\left[\left(1-\frac{z_0^2}{4a^2}\right)^{3/2}-1\right]. \tag{19}$$

The right hand side term in (19) is negative and corrects downwards the previous 2D approximation (11). In order to evaluate the accuracy of these approximate solutions, we now perform a numerical resolution of the Young-Laplace equation.

C. Numerical resolution

Eq. (7) was first normalized using the capillary length as the length scale ($Z = z/a$ and $R = r/a$) and split into two first

order equations

$$\begin{cases} F = \dot{R}, & \text{(20a)} \\ \dot{F} = Z[1+F^2]^{\frac{3}{2}} + \dfrac{1+F^2}{R}. & \text{(20b)} \end{cases}$$

Starting from an initial value of the height of the triple line $Z_{0,1}$ and for a given contact angle θ, we calculate an initial value of the radius of the triple line $R_{0,1} = \sqrt{Z_{0,1}(2B - Z_{0,1})}$ with $B = b/a$, of the angle $\beta_{0,1}$ using Eqs. (3) and (4) and of the slope of the meniscus $\dot{R}_{0,1} = -\tan\beta_{0,1}$ at the same place. The values of $R(Z + dZ)$ and $\dot{R}(Z + dZ)$ are calculated using a first order development. In order to converge rapidly, we chose for $Z_{0,1}$ the solution of Eq. (19) (Ferguson approximation) which slightly overestimates the real solution. Consequently, the asymptotic solution of Z when $R \to \infty$ is positive and the matching at the level of the liquid bath is not achieved. The algorithm is repeated with a decreased value $Z_{0,2} < Z_{0,1}$ and repeated until an acceptable solution is found at the horizontal liquid bath level. In practice we consider that the initial guess of Z_0 is accurate enough when the following conditions are met:

$$\text{for } R = 10,\ |\dot{R}| > 1000 \text{ and } |Z| < 10^{-2}.$$

This procedure was programmed in FORTRAN on a standard personal computer and converged in a few seconds. To illustrate the numerical method, we display in Fig. 2 the numerical profiles of the meniscus (the spatial coordinates are normalized by the capillary length a) in the case $B = b/a = 10$ and for contact angles in the range $0° \le \theta \le 90°$ corresponding to $-55.2° \le \beta_0 \le 25.4°$. In this figure we note that the sign of the slope of the meniscus profile can change when the liquid is wetting the solid surface (low θ values). In those cases, the meniscus presents a minimal radius smaller than the triple line radius. For non-wetting conditions (high θ values), the slope of the meniscus is always negative, and the triple line radius is the minimal radial extension of the meniscus. In Fig. 3 we represent in the plane (B, θ) the regions corresponding to both domains. The critical value θ^* of the contact angle separating both domains increases with B and presents an asymptotic value $\theta^* = \pi/2$. The profiles with a slope that changes its sign are obtained preferably for wetting liquids and large spheres. We now turn our attention to the determination of the height of the meniscus. In Fig. 4 we display the normalized height

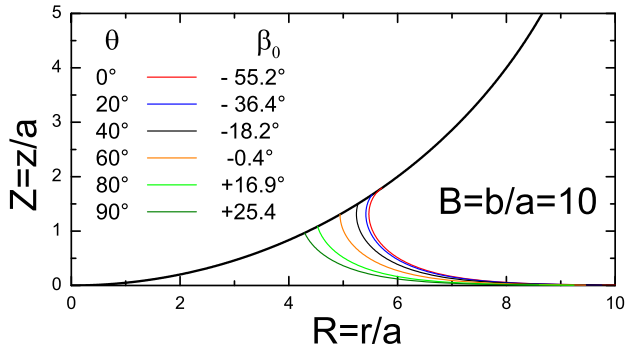

FIG. 2. Numerical meniscus profiles for $B = b/a = 10$ and $0° \le \theta \le 90°$ ($-55.2° \le \beta_0 \le 25.4°$). Z and R are the vertical and radial coordinates normalized by the capillary length a.

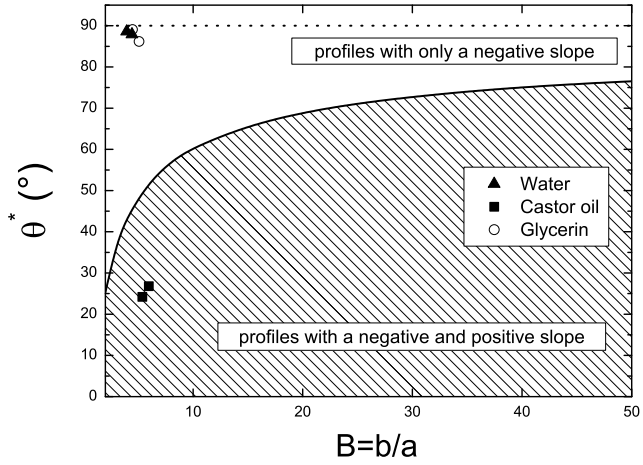

FIG. 3. Critical value of the contact angle θ^* vs $B = b/a$.

$Z_0 = z_0/a$ as a function of the normalized sphere radius $B = b/a$ for two contact angles $\theta = 20°$ (partially wetting material) and $\theta = 100°$ (non-wetting material). We note that the 2D approximation noticeably overestimates the numerical solution, whereas that of Ferguson appears to be in good agreement with the numerical solution. This is confirmed in Figs. 5 and 6 where the relative difference between the exact numerical solution and the solutions based on the 2D and the Ferguson approximations is given as a function of B for contact angles between $20° \le \theta \le 130°$. For the 2D approximation (Fig. 5), the relative difference is large, slowly decreases, and strongly depends on the value of θ. For the Ferguson approximation (Fig. 6), the relative difference rapidly decreases as B increases and seems to be relatively insensitive to the value of θ. As soon as $B > 2$, the solution of Ferguson (19) differs from the numerical one by less than 1% for all the contact angles less than 130°. Experimentally there is no smooth unpatterned surface on which such a high value of the contact angle can be found. For instance, for water and low energy hydrophobic smooth surfaces, the contact angles peak around 120°–130°.[21]

We conclude that the 2D approximation is too rough to accurately estimate the height of the meniscus (unless very large spheres are used: for instance for $\theta = 130°$, the

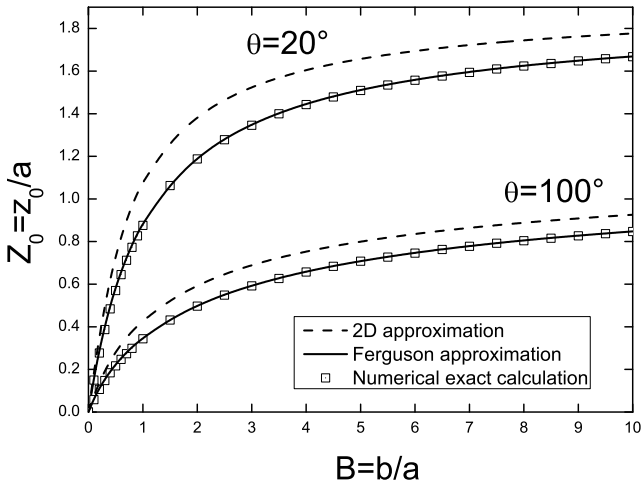

FIG. 4. Z_0 vs. B for $\theta = 20°$ and $\theta = 100°$.

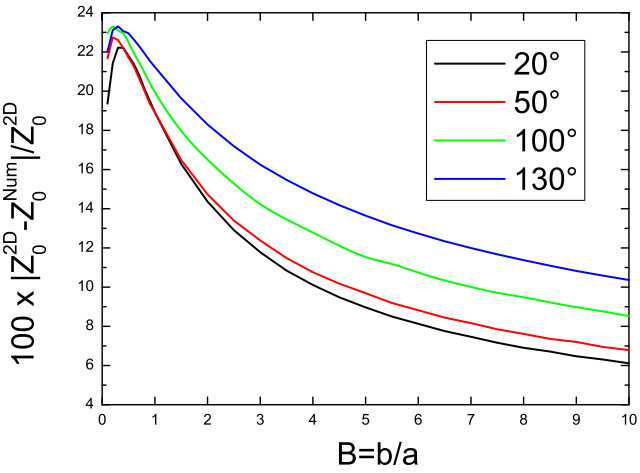

FIG. 5. Relative difference between Z_0^{Num} and Z_0^{2D} vs. $B = b/a$.

numerical solution and the 2D approximate solution are the same within 1% for $B > 1500$) and that the approximate solution of Ferguson is precise enough as soon as the sphere radius is only at least twice the capillary length. The latter being of the order of 2 mm for most liquids, the Ferguson approximation is sufficient for spheres of radius of the order of 4 mm. In the following, we use the Ferguson approximate Equation (19) to calculate the capillary rise onto a sphere instead of the numerical resolution of the complete Young-Laplace equation because it is much more straightforward (it is however also possible to use tabulated values or exact numerical values to fit the experimental data). From Eqs. (5) and (19), it is now easy to obtain σ (or $a = \sqrt{\sigma/\rho g}$) and θ independently if z_0 and p are measured. We have indeed from Eq. (19)

$$\sin\beta_0 = 1 - \frac{z_0^2}{2a^2} + \frac{4a}{3\sqrt{z_0(2b-z_0)}}\left[\left(1 - \frac{z_0^2}{4a^2}\right)^{\frac{3}{2}} - 1\right]. \quad (21)$$

And from Eq. (5)

$$\cos\beta_0 = \frac{p - \rho g \pi z_0^2\left(b - \frac{2z_0}{3}\right)}{2\pi\rho g a^2\sqrt{z_0(2b-z_0)}}. \quad (22)$$

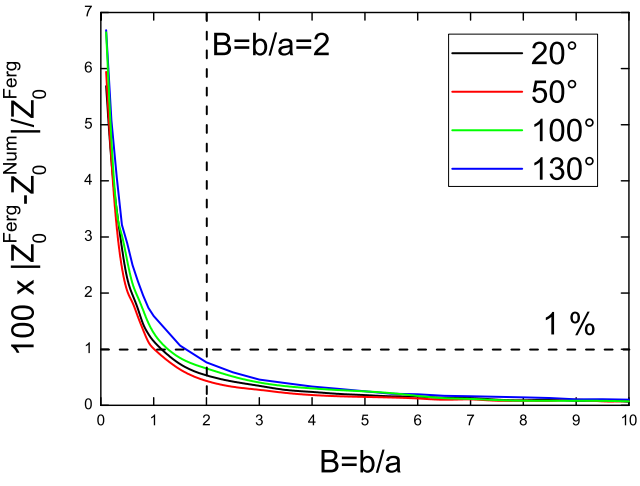

FIG. 6. Relative difference between Z_0^{Num} and Z_0^{Ferg} vs. $B = b/a$.

Eliminating β_0 in Eqs. (21) and (22), we obtain an equation for the variable a alone that can be solved numerically (we used the Wolfram Mathematica package) and the surface tension σ can be deduced. Once a is known, β_0 can be obtained from either (21) or (22) and the contact angle θ is calculated using Eqs. (3) and (4). In Sec. IV we experimentally test this new procedure by measuring simultaneously the force p and the height z_0 and applying the above equations to obtain σ and θ at the same time.

III. ACCURACY AND SENSITIVITY

The question of accuracy and sensitivity is of course of great significance in such a study. Due to the implicit and complex formulation, the uncertainty calculation for σ is difficult to perform using the Ferguson approximate solution for the capillary height z_0. It is however reasonable to suppose that it is of the same order of magnitude as the one obtained for the meniscus in the simpler 2D approximation. A numerical inspection of the two components of the force p in Eq. (5) reveals that they are of the same order of magnitude. Consequently, the order of magnitude of p is simply: $p \approx r_0\sigma\cos\beta_0$. Using the expression of the meniscus height in 2D approximation (11) and eliminating the contact angle β_0, we obtain for the surface tension

$$\sigma \approx \rho g z_0^2 + \frac{p^2}{\rho g z_0^3(2b - z_0)}. \quad (23)$$

A new inspection of both terms in (23) shows that the second term is prevailing. If the main uncertainties are those on p and z_0, the uncertainty calculation based on the second term of (23) gives

$$\frac{\Delta\sigma}{\sigma} \approx \frac{2\Delta p}{p} + \frac{3\Delta z_0}{z_0} + \frac{\Delta z_0}{2b - z_0}. \quad (24)$$

Using $\Delta z_0 = 16\ \mu$m and $\Delta p/g = 1$ mg as estimated in Sec. IV, we obtain a maximum relative uncertainty of the order of 3.4%. For the uncertainty concerning the contact angle, we can start again from the expression of z_0 in 2D approximation (11). By differentiating this expression, we have: $z_0 dz_0 = a^2\cos\beta_0 d\beta_0$. In our measurements (Sec. IV), the angle α varies little ($\Delta\alpha \approx 10°$ compared to $\Delta\beta_0 \approx 56°$) and we can approximate $\Delta\beta_0 \approx \Delta\theta$. The sensitivity of the method is thus

$$\frac{\Delta\theta}{\Delta z_0} \approx \frac{z_0}{a^2\cos\beta_0}. \quad (25)$$

Taking again $\Delta z_0 = 16\ \mu$m, we obtain for the measurements presented in Sec. IV, the uncertainties concerning the contact angle of the order of $\Delta\theta \approx 3°$ comparable to the other existing methods.

IV. EXPERIMENTAL VALIDATION

The sketch of the setup is presented in Fig. 7. Three common liquids were tested in order to validate the previous analysis: tap water ($\rho = 998$ kg/m^3), castor oil ($\rho = 962$ kg/m^3), and glycerin ($\rho = 1260$ kg/m^3). We used steel spheres from ball bearings (100Cr6 steel alloy) with radii $b = 10.15$ mm and

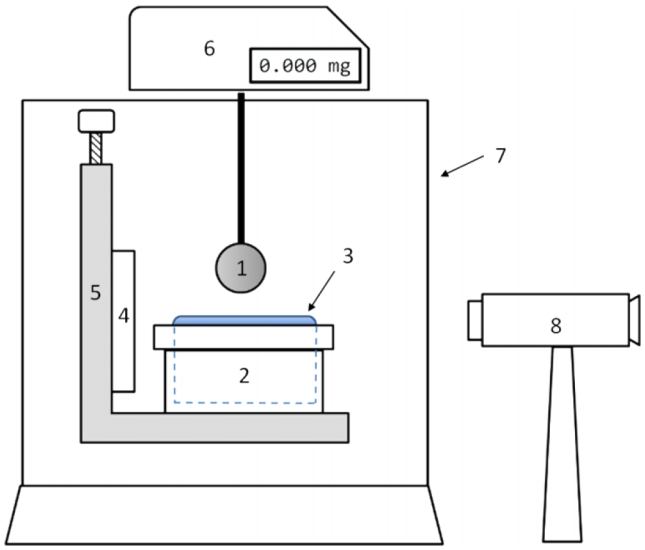

FIG. 7. Experimental setup: (1) sphere, (2) tank, (3) liquid/air interface, (4) backlight, (5) micrometric table, (6) balance, (7) glass box, (8) optical device (cathetometer or camera).

$b = 11.5$ mm. According to the manufacturer (CIMAP), the accuracy on their radius is of the order of 2.5×10^{-6} m. The spheres are fastened to the precision balance (model Kern PLJ, 1 mg read accuracy) by a rigid axis for the measurement of the force p. The height z_0 is measured by a cathetometer (10^{-5} m accuracy) or by image processing (Miro 4 camera from Vision Research and ImageJ software). A light-emitting diode (LED) backlight (OPT Machine Vision) is placed behind the sphere in order to obtain a contrasting image of the meniscus profile. The tank containing the liquid is the cup of a classical ring/plate tensiometer. Its radius is $R_t = 6$ cm and the liquid is filled to the brim so that the liquid interface slightly exceeds the top of the cup allowing one to easily see when the sphere touches the liquid. The tank is mounted on a vertically moving high precision motorized micrometric table (OWIS, 10^{-5} m accuracy, typical velocity 10 μm/s) to accurately control the height of the liquid surface. The whole setup is placed under a glass box to reduce disturbance and evaporation. The liquid temperature is measured before and after each trial. The main steps of the experimental procedure are as follows: the tank is filled with the liquid and the bottom of the sphere is detected by the optical device (cathetometer or camera). After the temperature is stabilized, the tank is lift up very slowly in order to minimize the interface riddles (especially for low viscosity liquids) and stopped when the bottom of the sphere reaches the air/liquid interface and the meniscus begins to form. The height z_0 at equilibrium and the force p are measured when the steady state is achieved (a few milliseconds for water and a few seconds for glycerin and castor oil, see below for the typical times of rising). In Table I, the measured values of z_0 and p are presented for the 6 trials. The measured force p_{mes} has to be corrected to account for the slight decrease in the tank level when the meniscus forms. Using the onservation of the liquid volume, the corrected force is

$$p_{cor} = p_{mes}\left(1 - \frac{r_0^2}{R_*^2}\right). \qquad (26)$$

TABLE I. Experimental parameters and results.

	Water		Castor oil		Glycerin	
b (mm)	10.15	11.50	10.15	11.50	10.15	11.50
T (°C)	23.1	22.8	23.8	24.2	22.3	22.4
z_0 (mm)	1.84	1.99	2.82	2.90	1.77	1.96
p_{mes}/g (mg)	285	347	344	409	305	385
p_{cor}/g (mg)	276	325	333	395	296	373
σ (mN/m)	64.66	64.27	33.60	35.11	63.59	63.56
a (mm)	2.57	2.60	1.89	1.93	2.27	2.27
θ (deg)	88.6	87.9	24.2	26.8	89.1	86.2

In the present tests, this correction is in the range $0.936 < 1 - r_0^2/R_t^2 < 0.970$. The measured meniscus height z_0 is also affected by the decrease in the liquid level in the tank but this correction is negligible (less than 0.8%). The last three lines of Table I give, respectively, the values of the surface tension σ, the capillary length a, and the contact angle θ deduced from the present analysis using the Ferguson approximate solution. The radial extension of the meniscus being of the order of the capillary length a, we have for all our tests $23 < R_t/a < 32$. Consequently, the edge effects can be reasonably neglected (the free surface of the liquid is perfectly flat at the center of the cup before contact and far from the meniscus when the capillary bridge is formed; consequently the shape of the meniscus depends only on the contact with the sphere). Moreover, the validity of the Ferguson approximation is also respected ($3.9 < b/a < 6.1$) justifying the use of Eq. (19) to obtain z_0. Within the experimental uncertainties, the values of σ are independent of the sphere radius and are in agreement with the values found in the literature. For each liquid we also used a pendant drop tensiometer (KRÜSS G10) to compare these values. The comparison is given in Table II. The relative difference between both methods is around 2% which validates our approach (the average value of σ of Table I is considered in Table II for the present method). From the knowledge of θ and σ, it is now also possible to reconstruct the shape of the meniscus using the numerical method described in Sec. II. Fig. 8 displays the superimposition of the real and numerically calculated menisci in the case of water and a sphere of radius $b = 11.5$ mm. The good agreement between both profiles gives confidence in the present technique. Experimentally we measure $z_0 = 1.99$ mm, the numerical calculation predicts $z_0 = 2.01$ mm and the solution of the equation using the approximation of Ferguson is $z_0 = 2.03$ mm. For water and glycerin, the experimental profiles have always a negative slope (the corresponding data are also plotted in Fig. 3) and the experimental determination of z_0 is easy. As noted in Sec. II (numerical section), it is also possible to observe menisci whose slope can change in sign when the liquid is wetting

TABLE II. Comparison of σ obtained by the present method and the pendant drop method.

σ (mN/m)	Water	Castor oil	Glycerin
Present method	64.5	34.4	63.6
KRÜSS G10	65.8	35.2	64.9
Relative difference (%)	1.98	2.33	2.04

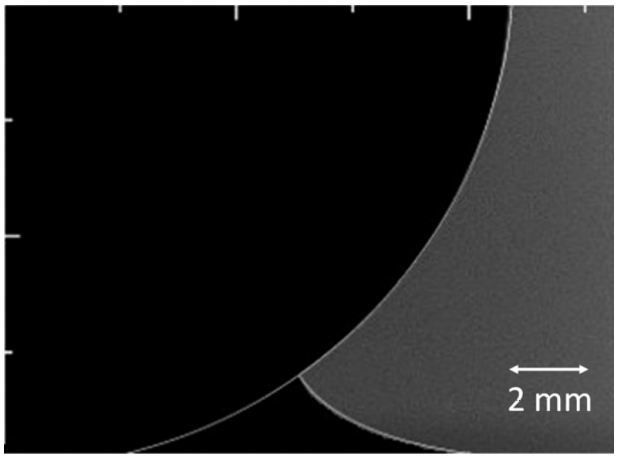

FIG. 8. Comparison between the experimental static meniscus and the theoretical shape (white line) derived from the numerical method for water and a steel sphere with radius $b = 11.5$ mm.

and/or the radius of the sphere is large compared to a. This is the case for castor oil as shown in Fig. 3. In those cases, the experimental measurement of z_0 requires special care. Moreover it is likely that the contact angle in the case of water is close to the advancing contact angle. Indeed as noted by Restagno[15] the capillary rise of the meniscus is very fast in the case of water and the final static contact angle may be close to an advancing contact angle. In fact following Clanet,[22] we estimate the time of capillary rise for water to be of the order of $t \sim \sqrt{\rho a^3/\sigma} \sim 16$ ms (inertial regime) and for castor oil and glycerin of the order of $t \sim 80\ \mu a/\sigma \sim 3$ s (viscous regime). These dynamic effects are important when the viscosity of the liquid is low and the surface tension is large. They are conveniently characterized by the Kapitsa number (comparison of the capillary force to the gravity and viscosity forces)

$$Ka = \left(\frac{\sigma^3}{\rho^3 g \nu^4}\right)^{\frac{1}{4}}. \tag{27}$$

This number is high in the case of water ($Ka \approx 400$) and low in the case of the castor oil and glycerin ($Ka \approx 0.3$) confirming that the contact angle is certainly close to an advancing contact angle in the case of water. For glycerin and castor oil the final contact angle is slightly different from the advancing contact angle. Finally the questions about accuracy and sensitivity have been discussed in Sec. III.

V. CONCLUSION

In this article we propose an alternative approach to simultaneously determine the surface tension σ and the contact angle θ contrary to all the other methods which require the knowledge of one of both parameters. This method is based on the measurement of the height z_0 of the meniscus on a sphere and of the weight p of the meniscus and the use of an appropriate model capable to relate these measurands to σ and θ. For this model, we adapt the Ferguson approximate solution (usually applied for the meniscus on cylindrical rods) to the spherical surface taking the sphere as the superimposition of cylindrical slices. This model allows us to calculate the static height z_0 of the meniscus on the sphere according to σ and θ. A numerical study clearly shows that the Ferguson model is very accurate as soon as the sphere radius is greater than twice the capillary length. As the present method is based on the measurement of z_0 and on the weight of the meniscus p we used a very simple experimental setup composed of a balance and a camera. Using different liquids and spheres, the successful comparison of our results for σ with the pendant drop method confirms the validity of this procedure.

ACKNOWLEDGMENTS

The authors would like to thank Pr. M. Souhar for our fruitful discussions and advice in this work.

[1] P. G. de Gennes, Rev. Mod. Phys. **57**, 827 (1985).
[2] P. G. de Gennes, F. Brochard-Wiart, and D. Quéré, *Capillarity and Wetting Phenomena: Drops, Bubbles, Pearls, Waves* (Springer, 2004).
[3] A. Marmur, Colloids Surf., A **116**, 55 (1996).
[4] A. W. Adamson and A. P. Gast, *Physical Chemistry of Surfaces*, 6th ed. (John Wiley & Sons, 1997), pp. 36–49.
[5] T. Young, Philos. Trans. R. Soc. London **95**, 65 (1805).
[6] L. Gao and T. J. Mc Carthy, Langmuir **22**(14), 6234 (2006).
[7] L. Léger and J. F. Joanny, Rep. Prog. Phys. **55**(4), 431 (1992).
[8] S. Y. Lin, H. C. Chang, L. W. Lin, and P. Y. Huang, Rev. Sci. Instrum. **67**, 2852 (1996).
[9] Y. Yuan and T. R. Lee, Springer Ser. Surf. Sci. **51**, 3 (2013).
[10] A. I. Rusanov and V. A. Prokhorov, *Interfacial Tensiometry*, Studies of Interface Science Vol. 3, edited by D. Möbius and R. Miller (Elsevier, Amsterdam, 1996).
[11] J. Drelich, C. Fang, and C. L. White, *Encyclopedia of Surface and Colloid Science* (Marcel Dekker, Inc., New York, 2013), p. 3152.
[12] K. J. Maloy, J. Feder, and T. Jossang, Rev. Sci. Instrum. **60**, 481 (1989).
[13] F. Zhu, R. Miao, C. Xu, and Z. Cao, Am. J. Phys. **75**, 896 (2007).
[14] A. D. Scheludko and A. D. Nikolov, Colloid Polym. Sci. **253**, 396 (1975).
[15] C. Huh and S. G. Mason, Can. J. Chem. **54**(6), 969 (1976).
[16] F. Restagno, C. Poulard, C. Cohen, L. Vagharchakian, and L. Léger, Langmuir **25**(18), 11188 (2009).
[17] C. Huh and L. E. Scriven, J. Colloid Interface Sci. **30**(3), 323 (1969).
[18] F. Bashforth and J. G. Adams, *An Attempt to Test the Theories of Capillary Action by Comparing the Theoretical and Measured Forms of Drops of Fluid* (Cambridge University Press, 1883).
[19] S. Hartland and R. W. Hartley, *Axisymmetric Fluid-Liquid Interfaces* (Elsevier, Amsterdam, 1976).
[20] A. Ferguson, Philos. Mag. **24**(6), 837 (1912).
[21] E. G. Shafrin and W. A. Zisman, Adv. Chem. **43**, 145 (1964).
[22] C. Clanet and D. Quéré, J. Fluid Mech. **460**, 131 (2002).